

**A New Magneto-Optic Based  
Flaw Imaging Device for  
Underwater Application**

**Final Report**

Prepared for

U.S. Department of Transportation  
Transportation Systems Center  
Cambridge, MA 02142

Prepared by

Failure Analysis Associates  
8411 154th Ave NE  
Redmond, WA 98052  
(206) 881-1807

January 1992

FaAA-SE-R-92-01-03

## Contents

Introduction.....	1
Technical Approach.....	2
Phase I Results.....	6
Phase II Technical Objectives.....	9
Phase II Results by Task.....	10
Conclusions and Recommendations.....	20
References.....	21
Appendix A - Test Report Underwater NDE Centre, University College London	

## INTRODUCTION

Underwater inspection of steel structures would be greatly facilitated by the development of simple, portable, devices for the direct visualization of flaws in the presence of marine fouling. Devices for use by a diver or devices that could be part of an automated submersible that could accomplish this task, would be a great benefit in many marine environments. This is especially the case for offshore oil platforms of all kinds and floating platforms in particular. But a versatile device of the type we propose would be useful in applications ranging from the inspection of ship hulls to drive shafts.

The investigation of ferrous materials by general electromagnetic methods has become a well established practice in materials research and in industry [1]. These methods can provide useful information about the tested object which includes the following:

- electrical conductivity  $\sigma$
- magnetic permeability  $\mu$
- electric permittivity  $\epsilon$
- thickness
- discontinuities (flaws, voids, cracks, and inclusions)

Other parameters may be accurately inferred from this information including case hardening, cold work, heat treatment or annealing status. Unfortunately, most electromagnetic tests are not well suited for rapid inspection of large surfaces or structures, and do not usually produce flaw images directly. All electromagnetic inspection techniques depend on some type of sensing device (pickup coils, Hall effect device, etc.) that responds to the electric, magnetic or electromagnetic field near the material specimen.

Often the sensing devices provide only crude indications of flaws, or require considerable data reduction before flaws can be fully characterized. The goal of this project is to promote a new class of electromagnetic field sensing device, namely magnetic garnet films [2,3], for the purpose of producing flaw images for ferrous materials in underwater applications.

Bismuth doped garnet films are potentially very sensitive to weak magnetic fields, and will rotate polarized light as a function of applied field strength. Garnet films have been designed and produced to have a switching field less than three gauss. This is the magnetic field that can switch the direction of magnetization in the entire film. Properly biased films up to four inches in diameter, or smaller portions thereof, can be switched in the presence of very weak magnetic fields, which, when added to the bias field, exceed the switching field. Owing to high potential sensitivity to weak magnetic fields (probably in the .01 gauss range) and to the demonstrated possibility of achieving high contrast magneto-optic visualization of the domain structure of the film [4], it is very likely that the weak magnetic fields associated with flaws in ferrous materials can be visualized using hand-held detectors of a design compatible with the needs of a human diver or an automated submersible.

The purpose of this research is to fully explore this basic concept, using a new optical sandwich design, and to demonstrate feasibility by actually constructing a device capable of

forming flaw images in ferrous materials. The new sandwich design would consist of an electroluminescent panel, garnet films and various other planar optical elements in a stack. Such a device would be capable of forming images of flaws even in the presence of marine fouling at distances of up to 1/4 inch. Because of the sandwich design, problems with deep water pressure compensation are eliminated. It would be applicable in areas currently investigated by devices employing magnetic particles in a watertight pouch. Unlike these techniques, direct instantaneous images of flaws would be available over large areas and at considerably high sensitivities using a far simpler hand-held device. This capability would provide a major new tool for inspection of underwater steel structures of any type, including ship hulls and especially offshore floating platform components.

## TECHNICAL APPROACH

The basic purpose of this work was to demonstrate the feasibility of using currently available magneto-optic materials (magnetic garnet films) to produce direct visual images of flaws near the surface of ferrous materials. This was to be accomplished using a compact hand-held sandwich device involving electroluminescent lighting and a variety of other planar optical elements in a stack. This technological development would represent a major advance in existing marine inspection technology.

In this section, we will briefly review the available techniques for producing flaw images in ferrous materials using existing garnet film technology. General magneto-optic imaging principles and general methods for forming images using these films will also be described. Once this background material has been presented, specific methods and tasks for achieving flaw images in ferrous materials using garnet film detectors in a sandwich design will be given.

### General Magneto-Optic Displays

Bismuth substituted iron garnets [2-4] possess a large specific Faraday rotation  $\theta_f$  which makes possible and practical both transmission and reflection mode magneto-optic displays of various types. A typical transmission mode display geometry is illustrated in Figure 1. If linearly polarized light is incident on a magnetic garnet film, the plane of polarization of the incident light will be rotated by an angle

$$\theta \propto \theta_f k \cdot M \quad (1)$$

where  $\theta_f$  is the specific Faraday rotation of the film,  $k$  is the wavevector of the incident light, and  $M$  is the local time dependent magnetization of the film at the point where the incident light passes through the film [4]. The sign of the scalar product  $k \cdot M$  determines the sense of the rotation. Note that in a solid, the Faraday rotation does not depend on the sign of the wavevector  $k$ , only on the angle between  $k$  and  $M$ . This means that the effect is doubled if a mirror or other reflective material is placed as shown in Figure 2. The mirror ensures that the beam will pass back through the epitaxial layer, thereby doubling the effective rotation of the plane of polarization.

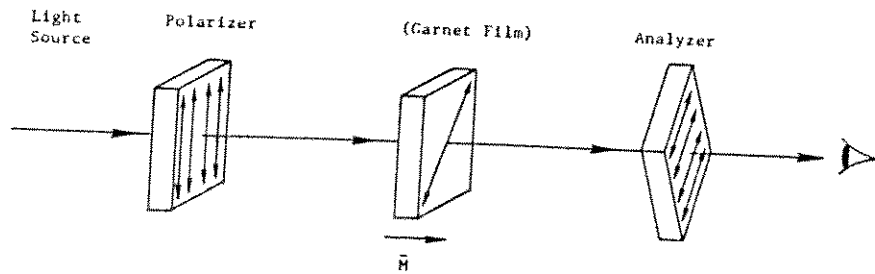


Figure 1. Basic elements of magneto-optic transmission mode display.  
The state of magnetization  $M$  in the garnet film is being observed.

The rotation of the plane of polarization of an incident, linearly polarized light beam serves as the basis of direct visualization methods. Ordinarily, in the absence of an applied field, domains (regions of uniform magnetization in the garnet film) are small. In many garnet films, especially those used in magnetic bubble memories, domains measure only several microns across [2]. However, in some garnet films the domains can be very large even when biasing fields are present [3]. In other materials, such as the material used in commercially available devices, small applied fields (three gauss or less) can cause the domains to coalesce into a single large domain several inches across. Such large domains allow perturbations due to flaws to be visualized provided the film has a sufficiently large specific Faraday rotation achieved with Bismuth doping [4].

#### A Pure Reflection Mode Device

Owing to the requirements for low lift off imaging (garnet film must be 'close' to the material because anomalies are weakened with distance) and the need to reduce surface light reflections from the garnet film, a general reflection mode display geometry of the general type illustrated in Figures 2 and 3 can be used.

Note that the reflection mode of operation, depicted in Figures 2 and 3, has many desirable features. The Faraday rotation produced by reflection is just twice that which is produced by transmission (see Figure 2). Moreover, there are generally two magnetic garnet films on the substrate separated by a short distance (.02 inches typically). This increases the effective film thickness by a factor of two, and thus improves flaw image contrast.

The problem with such a design (in a marine environment) is that the light source is at some distance from the garnet film and this inevitably leads to a box-like imager as shown in Figure 4. Such a box must either be sturdy enough to withstand significant pressures (at 200 ft., 100 psi) or be filled with a clear liquid and fitted with a pressure balancing membrane to balance the seawater pressure against the pressure of the liquid in the container.

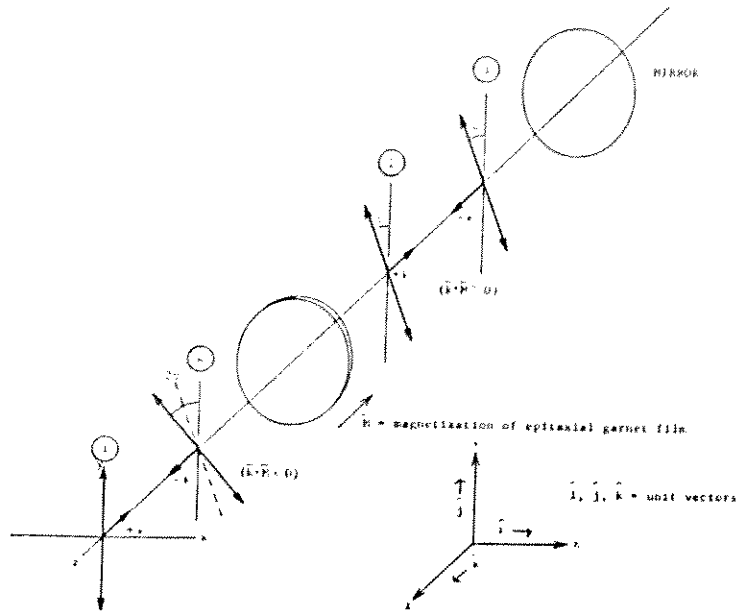


Figure 2. This figure illustrates the effect of a magneto-optically active garnet film on the plane of polarization of an incident light wave. (1) shows the incident light wave with wavevector  $k = -|k|\hat{k}$  along the negative z-axis and polarization along the y-axis. (2) shows a counter clockwise rotation of the plane of polarization due to passage of the light wave through the epitaxial garnet film. (3) shows the light wave (2) after reflection from a mirror and (4) shows the doubled Faraday rotation after the light wave of (3) passes back through the epitaxial film.

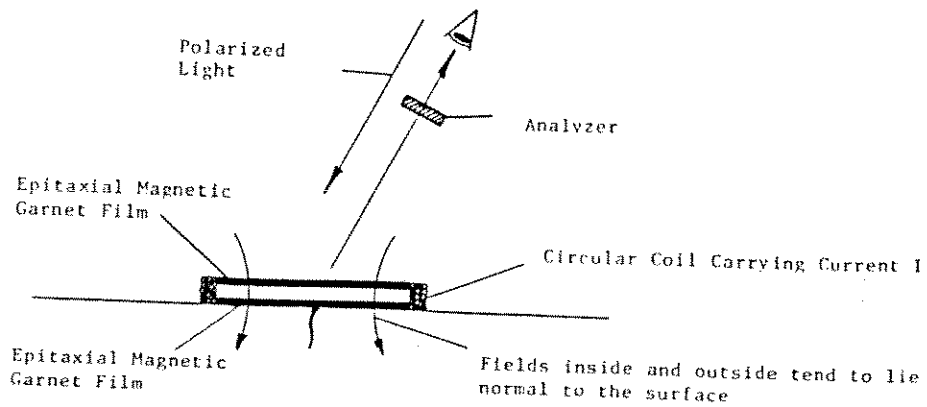


Figure 3. Basic reflection mode geometry for near contact imaging devices employing magnetic garnet films. Note that most films are deposited on both sides of the substrate.

Most of these difficulties could be eliminated by a new design which combines some of the features of a pure reflection design (Figures 2 and 3) and a pure transmission design (Figure 1).



Figure 4. MI-201-A Flaw Visualization Instrument. This box design would be eliminated using a new design involving a sandwich of garnet films, electroluminescent panels, polarizing materials and various internally reflecting surfaces.

In this project, we developed a sandwich design involving a garnet film and other optical elements which are 'backlighted' by an electroluminescent panel. Before describing this concept in detail, we will describe the state of the existing technology.

#### Ferrous Metals Inspection (An Existing Technology)

Spectron Development Laboratories (SDL) developed the first commercial magneto-optic based system for producing high resolution images of near-surface flaws in ferrous materials. This technology was ultimately purchased and further refined by Failure Analysis Associates Inc. [5-7]. The device (see Figure 4) employs a magnetic garnet film in an arrangement similar to that shown in Figure 3. In Figure 5, we illustrate a flaw image produced by the device using low frequency (60 Hz) time varying magnetic fields applied by a magnetic yoke. While this method of reflection imaging is successful for ferrous materials, under normal conditions, it is inadequate for imaging flaws in a marine environment.

#### The Sandwich Design

One concept for a sandwich design is illustrated in Figure 6. It is clear from this figure that the new sandwich design is a hybrid involving both transmission of light through the garnet film (one way) and multiple reflections through the film (analogous to the pure reflection mode of Figure 2). An electroluminescent panel is similar to a capacitor in that it consists of dielectric material between two conducting surfaces. A luminescent pigment is dispersed within the dielectric material and subjected to the electrostatic field of the charged capacitor.

If an AC voltage is applied across the panel, the phosphor particles will be in a continuing state of excitation giving off a steady light in the form of a glow. For panel lighting applications, one plate or electrode of the panel is translucent to allow transmission of the light.

Since the light phenomenon occurs by a means other than the temperature of the source, it fits the definition of luminescence. Since the source of the excitation is an electric field, the panel is electroluminescent. The electroluminescent panel requires approximately 130 Vac at 400 to 1000 Hz for excitation. An inverter that operates from a 5 Vdc source is possible. Unless some method of compensation is provided, the light output of the electroluminescent panel will decrease with age. By incorporating the panel's capacitance as a part of the inverter circuit, the voltage and frequency output will be changed to properly compensate for the panel's aging and maintain an essentially constant light output.

The electroluminescent panel has a limited light output and this light must be used as efficiently as possible in forming a high contrast image of a flaw. Figure 6 shows a sandwich design consisting of two partially reflecting surfaces (partially reflecting front surface mirrors in effect), a source of light (electroluminescent panel), the garnet film (two epitaxial layers on a nonmagnetic substrate) and two sheets of polarizing material. The most efficient design is one that maximizes both the light intensity and the image contrast. These happen to be somewhat conflicting requirements since contrast is maximized by multiple internal reflections while intensity depends on the amount of light which leaks out of the sandwich [8].

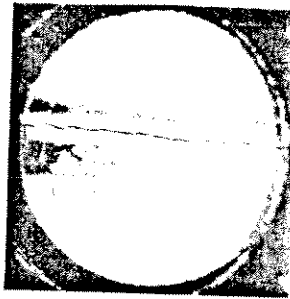


Figure 5. Image produced by the MI-201-A is a tight nonvisible crack in a steel bar (cross section 2 in. x 2 in.) possessing a long sinuous longitudinal crack. A 115 volt, 50 Hz yoke supplied an external low frequency excitation field  $B(t)$ .

### PHASE I RESULTS

During Phase I, we produced a simple prototype device having the general features of the final system. However, for the purposes of the Phase I feasibility demonstration; we decided to keep the design as simple as possible by eliminating the front surface mirrors. The design we chose is illustrated in Figure 7. It consists of a commercially available electroluminescent

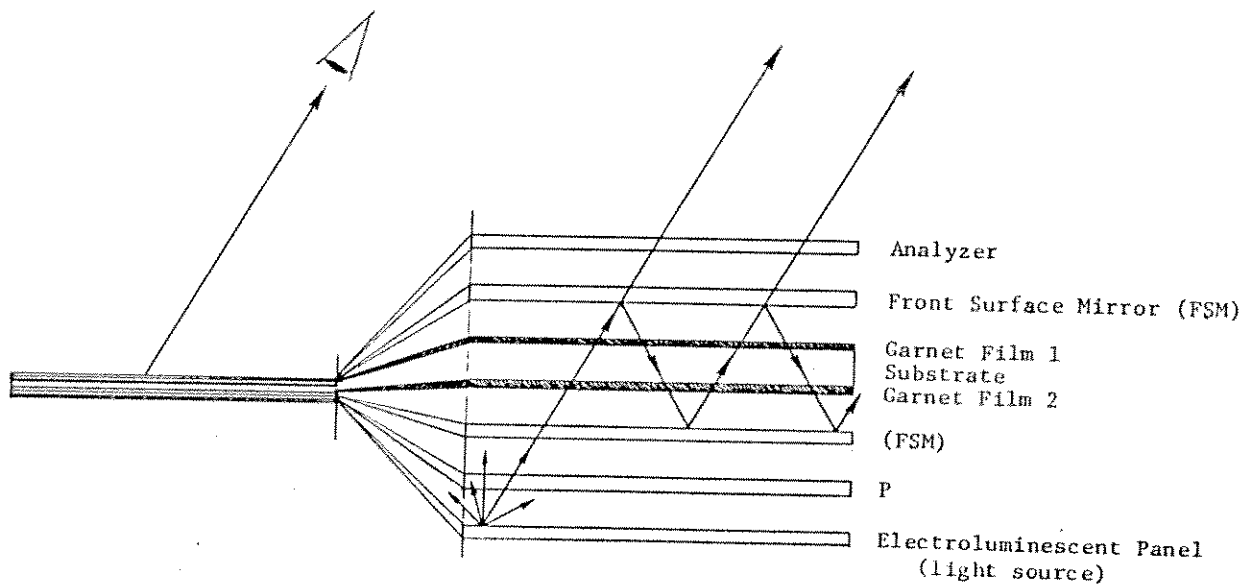


Figure 6. This design has two partially reflecting mirrors on either side of two epitaxial garnet layers. Note that light from the light source passes through a polarizer, then passes through the entire stack and reflects from the back of the mirror above the garnet films, back down through the garnet films and again reflects from the mirror below the garnet films. This happens a number of times and some of the light from the light source eventually leaks out of the stack reaching the viewer.

panel (aircraft green) measuring 1/16 inch thick by 3/4 inch wide by 2 inches in length, a garnet film (.02 inch thick) and two pieces of Polaroid (HN42). A small coil form surrounding this rectangular stack was constructed and 100 turns of #32 copper wire was wound on the form. A circuit was designed to drive the coil and the device illustrated in Figure 8 was assembled.

The coil drive circuit generates a waveform that sensitizes the crystal and erases the prior image. By choosing a low duty cycle, it was possible to operate the device on four AA size alkaline batteries (1.5V). Power for both the electroluminescent panel (1000V DC) and the coil surrounding the optical stack was supplied by these cells.

Experiments with this device indicated that it worked very well. The intensity of the electroluminescent panel was sufficiently bright that images could be seen under most ambient light conditions (except direct sunlight). However, the electroluminescent panel was too thick to get good images of certain flaws. This is not a crucial concern where large (long) cracks are involved, but it was decided that thinner panels would be desirable. Moreover, the system was not watertight. Having demonstrated that a simple prototype worked we set out to increase its size and make it watertight.

There are two competing aspects of the images produced by this device, namely image intensity and image contrast. Unfortunately, the electroluminescent panels are not terribly bright light sources. Moreover, when the optical elements are potted in epoxy, there is a tendency to reduce the light that is transmitted through the system owing to multiple internal reflections.

If one adjusts the light intensity to be a maximum (by adjusting the polarizer) it happens that the contrast (intensity difference between a north pole and a south pole) in the image is greatly degraded or nonexistent. Conversely, if one adjusts the contrast to be a maximum, the intensity is greatly reduced. This can be compensated either by increasing the voltage to the electroluminescent panel (which shortens its lifetime) or by sacrificing contrast.

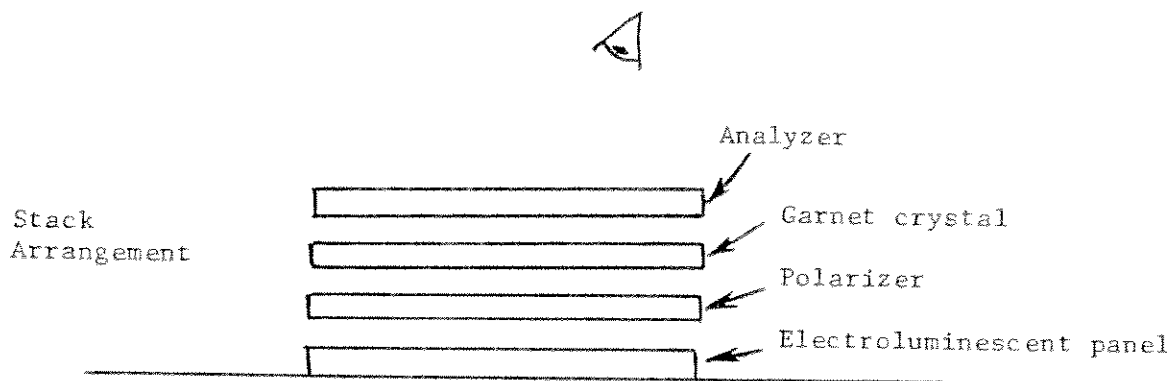


Figure 7. Basic experimental arrangement developed designs Phase I.

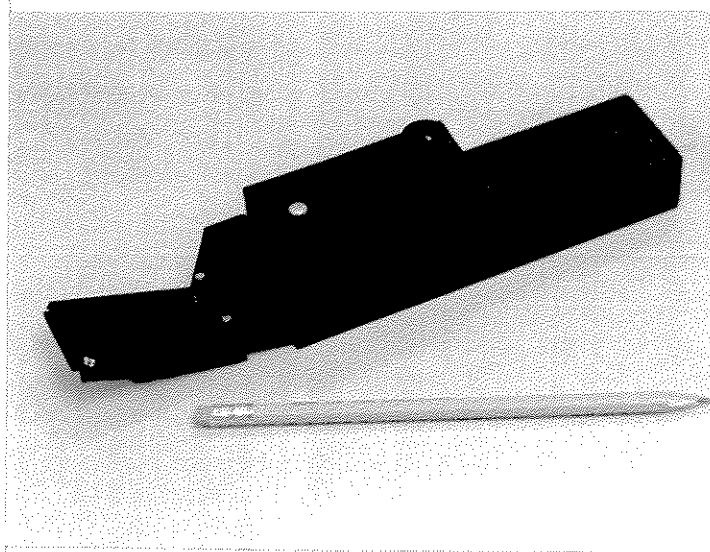


Figure 8. Prototype Underwater Flaw Imager.

Experiments with the system suggest that contrast is important and that intensity (especially in an underwater environment where it is often dark) is less important. In any case there are good reasons for expecting that brightness can be improved by increasing voltage to the electroluminescent panel as mentioned above.

## PHASE II TECHNICAL OBJECTIVES

The objectives of the Phase II program were to fully assess the feasibility of developing an underwater flaw imaging system that meets the stated needs of the U.S. Coast Guard and other users. To meet these objectives, the Phase I prototype was redesigned to withstand the rigors of actual use in an underwater environment. The specific objectives for Phase II were:

1. Determine if the materials currently used (epoxys, plastics, etc.) will withstand the conditions of temperature and pressure expected. It is particularly important to determine if changes in temperature and pressure will affect the potted crystal. That is, will stresses cause cracking? It is also important to determine if the corrosive environment of seawater will be a problem for any of the proposed materials.
2. Determine if the currently configured device is compatible with the anticipated needs of the user(s). It is recognized that such devices may be used in a number of different ways by a number of different users. Each application will require that the structural component be properly magnetized in order to insure that a flaw has been found. This is crucial if the flaw imager is to do its job.
3. Transfer this technology to the user(s) in the forms most desirable to them. It is anticipated that the device may take differential final forms for different applications. For example, the shape of the viewing window can be altered to fit into special areas for special inspections.
4. Determine what kinds of documentation best suits the user(s). In many cases the only requirements will be to find a crack and mark it with an appropriate indicator for later repair. In other cases, detailed photographic or other documentation will be needed.

These objectives included plans to work closely with individuals familiar with the requirements for underwater inspection.

## PHASE II RESULTS BY TASK

### Task 1- Identify Problems to be Solved and Acquisition of Specimens.

In attempting to identify the type of uses the imagers would be put to and the environment in which they would operate, we contacted individuals and companies involved in underwater inspection. We discussed the project with J.P. Kenny and Partners Ltd. of the United Kingdom. J.P. Kenny was acting as a research manager for a program sponsored by a consortium of oil companies and the U.S. Coast Guard. We also arranged for a prototype imager to be tested by the Underwater NDE Centre which is affiliated with the Department of Mechanical Engineering of University College London. The scope and results of these tests are discussed in the section on Task 5.

We have assembled a variety of specimens and samples for testing the prototype imagers under laboratory conditions. These samples include a set of steel plates and pipe sections with simulated cracks of various sizes and orientations. We have also obtained a pipe removed from an operating oil field. This pipe contains a large crack that we successfully locate using the prototype imagers. This pipe section was provided to us by AMF Tuboscope. All of these samples have been used to evaluate the performance of the prototype imagers under a variety of conditions.

### Task 2 - Materials and Environmental Tests.

During the Phase I program we used five magnetic garnet films to build prototypes. Not all of these films resulted in successful imagers. Some were broken due to the potting procedures and removal from molds. Others did not have sufficient image intensity or contrast to be useful (due to the settings on the polarizers). In short, there are many variables to consider when designing the imagers and errors were inevitable.

The epoxy we selected to fabricate the Phase I prototypes proved to be excessively brittle. As a result, we were concerned that the stresses associated with temperature and pressure changes in the underwater inspection environment would damage the imager. Consequently, we began an investigation to identify an epoxy with characteristics more suitable for this application. Our testing indicated that the epoxy DC 140, manufactured by Thermoset Plastics Inc. of Indianapolis Indiana, had physical properties that met our specifications for this application. DC 140 is a two part water-clear epoxy that is both resilient and resistant to the corrosive effects of salt water. Using this epoxy, we fabricated several simulated imagers and successfully tested them in a variety of environments, including off shore submersion to a depth of 900 feet in saltwater as described in Task 5 results.

Under this task, we also studied the corrosion characteristics of the materials used to fabricate imagers. To perform this study, we obtained an aquarium which we filled with salt water. A bubbler was placed in the aquarium to oxygenate the water. We placed a prototype imager in

this salt water bath for 30 days. After removing the imager, we performed a thorough evaluation of the unit and found that it had suffered no damage. Further testing of the imagers in both salt and fresh water was conducted in Task 5.

### Task 3 - Obtain a New Source of Magneto-Optic Crystals.

In this task, we investigated alternatives to the magneto-optic garnet films that are used in the imager. There were several reasons for investigating alternatives: First, the garnet film is a manufactured material with very few other uses and consequently it may be difficult or impossible to obtain additional quantities of the film in the future (our original supplier for the film, Allied Technology of Charlotte, North Carolina has decided to quit making the crystals). Second, the film is very rigid and consequently cannot easily be used on curved surfaces. As will be discussed in Task 5, this problem was one of the main criticisms of our current imager. In order to address these problems, we began a search for alternative techniques to image magnetic field lines.

The most promising device we investigated involved an application of liquid crystal display technology. Basically, this device uses a liquid crystal material doped with magnetic particles. When the device is turned off, the liquid crystal molecules are randomly oriented so that the viewer is opaque. When switched on, the liquid crystal molecules align and light can be transmitted through the viewer. Doping the liquid crystal molecules with magnetic particles should cause the molecules to become unaligned when the magnetic particles interact with an external magnetic field. Figure 9 shows how this effect would work.

As shown in Figure 9a, when the magnet particles are exposed to a uniform magnetic field, they form long chains. These chains form perpendicular to the orientation of the liquid crystal molecules when the electric field is switched on. In this orientation, the magnetic particles do not affect the transmission of light through the viewer. However, as indicated in Figure 9b, when the magnetic field is disrupted by a crack or other defect, the disruption changes the alignment of the chains of magnetic particles. In theory, the movement of the magnetic particles will also move the liquid crystals molecules out of alignment causing localized areas on the viewer to become opaque. The areas on the viewer that become opaque are thus related to anomalies in the magnetic field and hence to cracks in the component.

Building the underwater imagers using this approach would have a number of benefits over using our current garnet film technique. Since liquid crystals are used extensively in laptop computers, wrist watches and a myriad other devices, it is unlikely that it would ever be difficult to obtain the material. Also the devices can be made very flexible. For example, Edmund Scientific currently sells large area (1 foot by 3 foot) liquid crystal light shutter windows (Stock No. N37,541). These devices consist of a liquid crystal emulsion spread between sheets of conductive plastic film. The plastic film makes these windows extremely flexible and as a result, they could easily be made to conform to curved piping components.

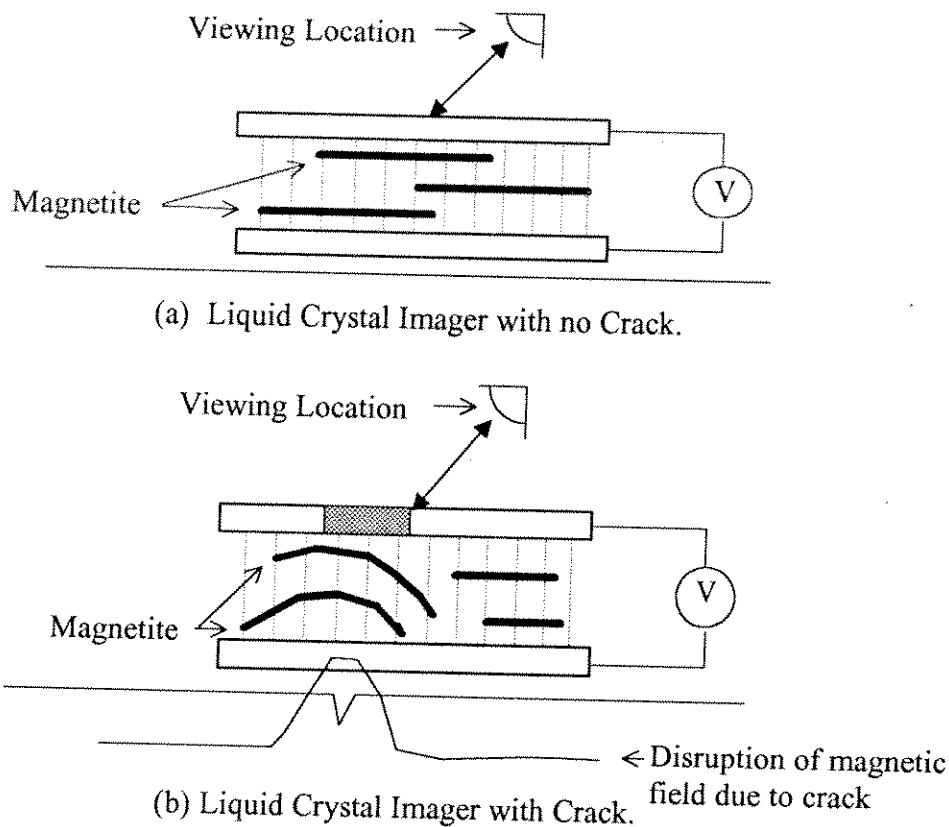


Figure 9. Theoretical Operation of Liquid Crystal Imager.

We attempted to build several liquid crystal devices that would be sensitivity to magnetic fields. The first hurdle in designing these devices is to determine the amount of magnetic material to add to the liquid crystal. Too few magnetic particles would not have the desired effect on the transmissivity of light while too many particles would inhibit the transmission of light by the liquid crystal molecules. The optimum number of magnetic particles to use must therefore be determined experimentally. We conducted a number of experiments in an attempt to quantify the required doping but were unable to achieve satisfactory results.

The procedure we developed to fabricate liquid crystal sensors which are responsive to magnetic fields is as follows:

1. Prepare ferric-oxide needles (magnetic particles)
  - a) Coat ferric oxide with a 0.1% solution of DMOAP
  - b) Remove DMOAP using a strong magnet to hold the needles in place while removing the liquid.
  - c) Dry in an argon atmosphere for 1 hour.

2. Clean the substrate (glass plates with a transparent conductive coating on one side) with Sparkleen and rinse with distilled water.
3. After thorough rinsing, clean the substrate with chromic-sulfuric acid cleaning solution. **CAUTION**, this cleaning must be performed under the fume hood.
4. Agitate the substrate in a 0.1% solution of DMOAP for five minutes and then rinse thoroughly with distilled water. Blow dry with N<sub>2</sub> or argon gas and cure in an oven for 1 hour at 100 degrees C.
5. Place substrate on a table with the conductive side face up. Dust the substrate with fiber optic fibers using a powder blower. Avoid breathing the fibers.
6. Coat the edges of the substrate with UV curing adhesive (Norland Optical Adhesive 61) leaving a 1/2-inch opening on one side (for subsequent insertion of liquid crystals).
7. Place the second substrate on the top of the first with the conductive layer face down to form the cell. If the buss bar on the bottom substrate is on the right side of the cell, the buss bar on the top substrate should be on the left side. Leave a gap the size of the buss bar on either side of the cell to facilitate lead-wire attachment.
8. Place the cell under a UV lamp and allow to cure.
9. Hang the cell upside down in the vacuum chamber. Place a combustion boat one half full of liquid crystal (Licristal ZLI-3497-000 or ZLI-3700-000 manufactured by EM Chemicals) doped with the ferric oxide from Step 1 in the chamber.
10. Draw a vacuum and lower the cell into the combustion boat. Restore air pressure to the vacuum chamber. This will force the liquid crystal into the cell. Repeat this cycle at least three times to fill the entire cell.
11. Remove the cell from the chamber and lay it on a vacuum plate. Cover the plate with a plastic sheet except in the vicinity of the 1/2-inch opening.
12. Apply a vacuum to the plate to force out some of the liquid crystal, wipe off the excess and seal the hole with UV adhesive. Place the cell under the UV lamp and allow to cure.

As this procedure indicates, the process of fabricating liquid crystal magnetic sensors is both complex and time consuming. Due to this complexity, Phase II program resources were insufficient to complete the number of experiments necessary to determine the optimum fabrication parameters. We also encountered problems with clumping as we increased the concentration of ferric-oxide particles added to the liquid crystal. The DMOAP coating of the ferric oxide in Step 1 was an attempt to reduce this tendency to clump. However, as the concentration increased, the DMOAP coating had less and less effect. A point was quickly reached where the clumping clogged the cell access port prevented the liquid crystal from entering the cell. As a result, we were unable to reach the ferric-oxide concentrations where the magnetic field interaction with the liquid crystal molecules could be observed.

At low ferric-oxide concentrations we were able to load the cells successfully. Examination of these cells under the microscope showed that the ferric-oxide particles formed long chains when exposed to a magnetic field. This result was as expected by the theory. When the magnetic field was perturbed, the ferric-oxide chains would move in response to the change. However,

because the concentration of ferric-oxide particles was so low, there was no visible effect on the transmissivity of the liquid crystal. We did find that the response of the liquid crystal to an applied electric field was not affected by the addition of the ferric-oxide particles, at the concentration levels we were able to achieve. This fact suggests that a magnetic field sensor based on this approach is indeed feasible. However, substantial additional work would be required to realize such a sensor.

In undertaking additional work on sensors of this type, we would propose to work closely with a manufacturer of liquid crystal displays. Several manufacturers have developed liquid crystal emulsions that are painted on conductive surfaces. Using this type of liquid crystal would greatly simplify the fabrication of test cells. Unfortunately, we were unable to obtain any of this material. The liquid crystal manufacturers we spoke with indicated that they prepare the liquid crystal emulsion themselves using proprietary techniques. For this reason, we feel that identifying a manufacturer to work with would be a tremendous benefit in terms of access to the liquid crystal emulsion and to their extensive knowledge base.

We feel that magnetic field imagers based on ferric-oxide doped liquid crystal could have significant advantages over the garnet film approach particularly in terms of availability of raw materials and ability to bend and form the sensors to inspect piping and other unusually shaped structures. We strongly recommend that the Department of Transportation fund additional work in this area in order to ascertain the commercial feasibility of these sensors.

#### Task 4 - Construction of Phase II Imagers.

Three prototype imagers were constructed using garnet films during Phase II. The new imagers were constructed using larger thinner electroluminescent panels that were also waterproof. The new design also employed full size three inch diameter garnet films to provide a larger viewing area. The coil drive circuit developed during Phase I was also modified to utilize lithium rechargeable batteries.

Prior to constructing the imagers, we conducted a variety of experiments to determine the optimum fabrication techniques. The first step in this process was to machine several Teflon molds. Examples of two of these molds are shown in Figure 10. The fabrication process was developed to some extent through trial and error building on the results of our Phase I work. The Teflon molds are used in the construction of the optical stack. The process begins by assembling the stack and fitting it into the mold. The mold is then filled with epoxy which serves as a bonding agent and a waterproofing medium. The entire assemble is then placed in a vacuum chamber to remove all air bubbles trapped between the optical layers. After a period of between five to fifteen minutes under full vacuum, the air pressure in the chamber is gradually returned to normal. The gradual increase in air pressure, which takes about one minute, allows the epoxy to fill the voids. After some experimentation, we learned how to prepare optical stacks with very few entrapped bubbles or other defects.

During Phase I we had encountered significant difficulty removing the optical stacks from the Teflon molds. Often the garnet crystal would break or the epoxy would shatter. However,

using redesigned molds and switching to the DC 140 epoxy (discussed in Task 2), we were able to eliminate these problems in Phase II.

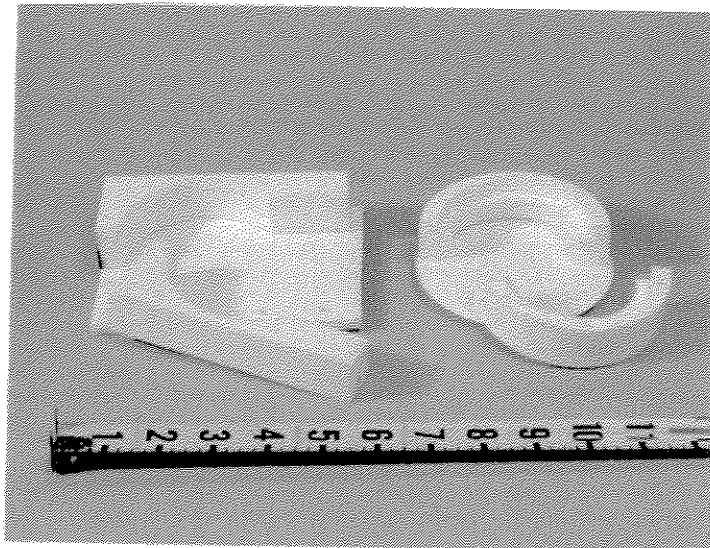


Figure 10. Teflon molds used in fabricating the optical stacks.

The next step in the fabrication process involves inserting the optical stack into a coil form, winding a 100 turn coil (#21 copper wire) measuring five inches in average diameter around the stack (3 1/4 inches in diameter), and inserting this combination in a second Teflon mold for a second potting operation. This second operation, like the first involved removal of the air in the coil and in the spaces between the optical stack and the coil form. Epoxy flowed into these void spaces as the pressure in the vacuum chamber was slowly returned to one atmosphere. At the completion of this second potting operation, the optical elements and energizing coil were contained in a single watertight unit.

The first two imagers built during Phase II had a six inch diameter framework surrounding the 2 3/4 inch active viewing area. The framework provides support for the optical stack as well as the energizing coil that surrounds the stack. Photos of the two prototype units are shown in Figure 11. The imager is hand-held and battery operated. The optical stack and energizing coil are attached to a flashlight like tube that houses the control circuits. Batteries were housed in this tube and the tube was fitted with watertight seals for shallow water operation. A watertight on-off switch for use in shallow water was also provided in the unit. Fabrication of these two prototypes provided valuable experience working with the epoxies and fabricating the optical stack. The large framework simplified the assembly process by providing space to mount the components. However, we realized that the large diameter would severely limit the use of the imager in the vicinity of tees and wyes. Consequently, we initiated an effort to minimize the structure surrounding the viewing area without compromising the strength of the unit.

Figure 12 shows several of the simulated optical stacks we constructed. These units were assembled in order to develop the fabrication techniques we would need to construct smaller more compact imagers. Based on this work, we were able to fabricate the third prototype imager shown in Figure 13. In designing this unit, we tried to anticipate possible field uses of

the imager. As shown in the figure, this imager has a much smaller framework supporting the optical stack. This reduced size permits the imager to be operated much closer to tees, wyes and other obstructions. As with the earlier two Phase II prototypes, the flashlight-like tube contains the electronic circuits and batteries. This unit also has a watertight on-off switch suitable for shallow water operation. For deeper water operations, we would replace the watertight switch with a small external magnet and a Hall-effect device inside the tube. This arrangement would provide a switch that requires no mechanical connections to the interior of the tube.

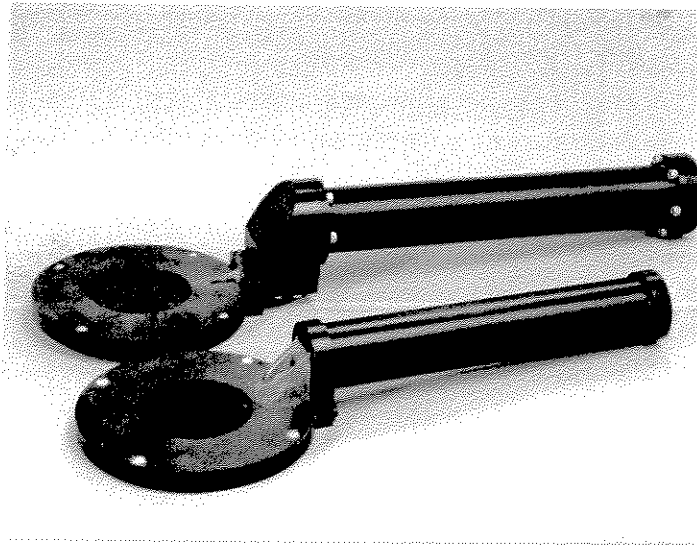


Figure 11. Prototype imagers with large supporting framework around optical stack.

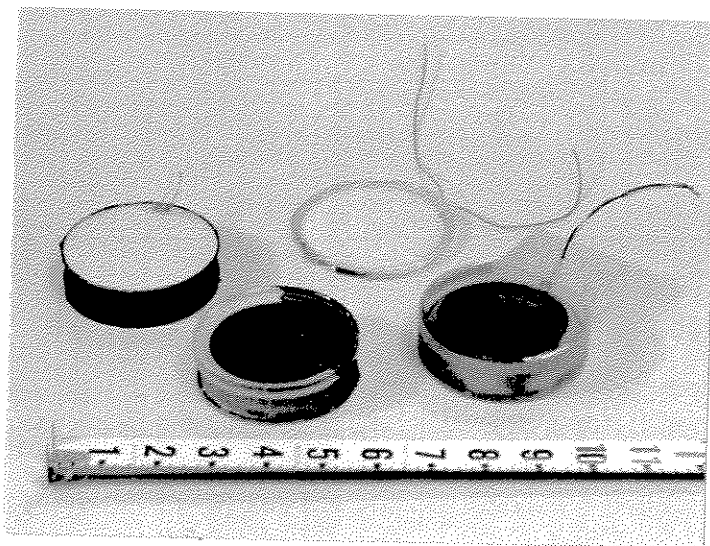


Figure 12. Simulated optical stack components for final Phase II prototype imager.

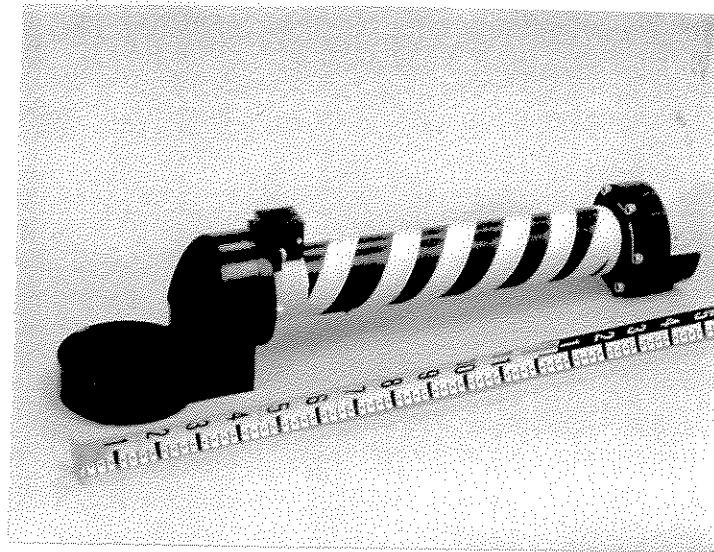


Figure 13. Phase II prototype imager with compact optical stack.

#### Task 5 - Experiments.

A variety of experiments were conducted to evaluate the prototype imager's performance in the field. As mentioned in the discussion of Task 2, we exposed one of the units to a corrosive salt water environment for 30 days with no apparent damage. In addition to these tests, we also conducted tests to determine if the units could withstand the temperatures and pressures associated with underwater operation. We conducted a series of three tests. The first test was designed to evaluate the performance of the imager in shallow salt water. For this test, we lowered the imager to a depth of 40 feet in salt water. After the unit was removed from the water, we found that it was working properly and that no water had leaked into the interior.

After the success of this first test, we felt sufficiently confident in the design to subject the imager to much higher pressure. For the second test, we lowered the unit to a depth of 200 feet in Lake Washington. After removing the unit from the water, we again found that it was

functioning correctly and that no water had leaked into the mechanism. For our final test in this series, we lowered the imager off a boat in the middle of Puget Sound. In this test, the imager was lowered to a depth of 900 feet. We felt that this depth was well in excess of the depth that the imager would experience in normal use. Therefore, survival at 900 feet would provide a comfortable margin for safe operation of the imager. After retrieving the unit from depth, we found that the imager was operating properly and that no water had leaked into the unit. Based on these results, we were confident that our design could survive the rigors of underwater use.

Following the successful completion of the survivability test, we felt the prototype imager was ready to be tested in actual operation. To perform these tests, we turned to the Underwater NDE Centre which is affiliated with the Department of Mechanical Engineering of University

College London. Our point of contact at the Underwater NDE Centre was Mr. John Rudlin. A copy of his evaluation of one of the prototype imagers is included in Appendix A. Briefly, this report contained the following findings:

#### Flat Plate Tests

The imager was able to detect cracks and/or slots on flat plates. Figure 14a shows the imager being used to inspect a visible slot. The slot dimensions are 0.15" wide by 0.1" deep. Figures 14b and 14c show the imager inspecting visible cracks in a grounded weld bead. In all three figures, the crack being inspected by the imager is visible. However, if the surface of the component is obscured by biofouling, the defects could be detected by the imager even if they were not visible. Findings also suggest that cracks in slightly convex surfaces may also be detectable although the magnetic field may be more difficult to set up. The device is very sensitive to orientation of the external magnetic bias field, and it is suggested that an improved and simpler operation could be obtained with a field supplied from the device itself. As shown in Figure 14d, a raised weld bead has obscured signals from a large slot, suggesting that the imager cannot readily be used for crack detection when a raised weld bead is present.

#### Tubular Joint Tests

Several attempts were made to inspect tubular joints but in no case was it possible to obtain signals from cracks, even when the crack was large enough to be visible with the naked eye. The reason for this is that the angle of the weld bead and/or the angle of the joint prevents access of the instrument to the area where the magnetic field has been disturbed by the crack.

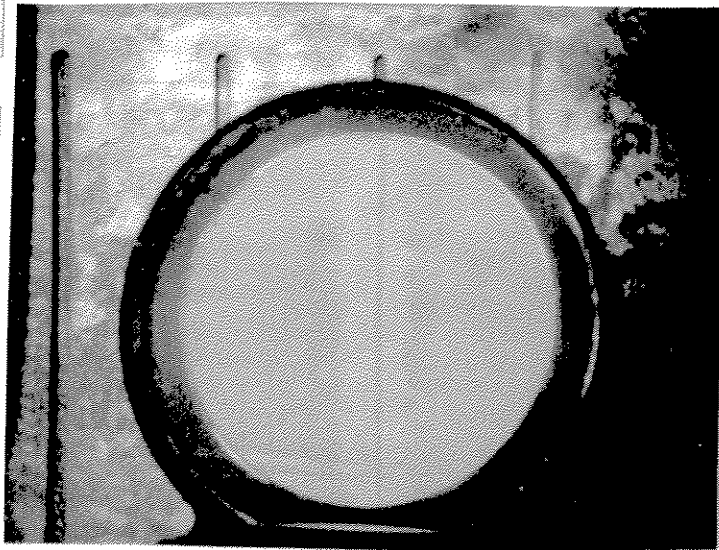
#### Underwater Operation

No problems were experienced with underwater operation of the device other than setting up of the magnetic field.

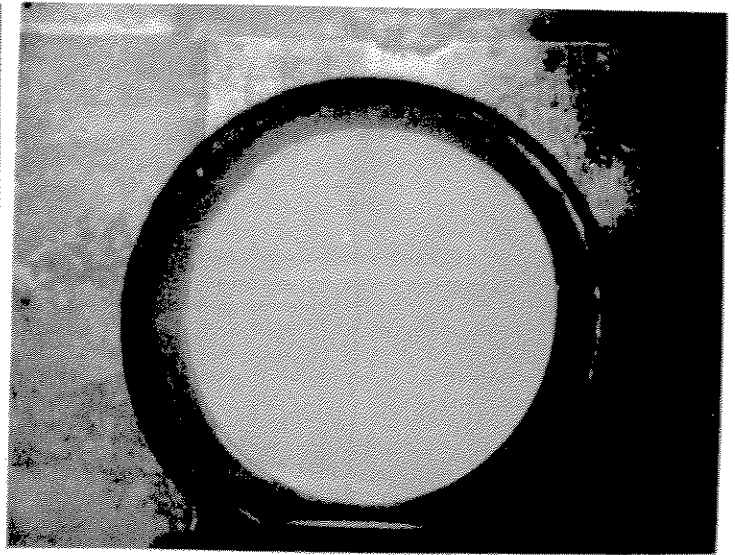
The Underwater NDE Centre concluded that "The device is capable of detecting cracks in flat plates underwater, but is generally unsuitable for welded joints in the as welded condition." The Underwater NDE Centre recommended the following modifications to the device:

1. Incorporate a magnetic bias field generator into the device.
2. Reduce the size of the sensing area so that it will fit into weld toes and angled joints.

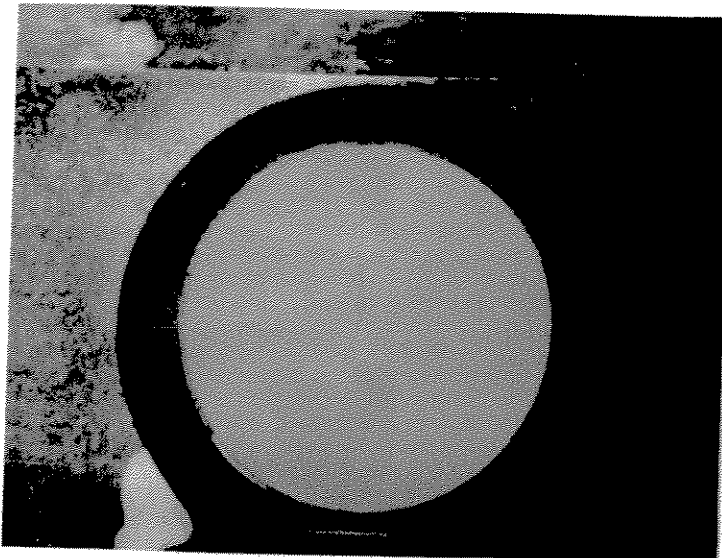
We concur with both of these recommendations. If we undertake Phase III work, we intend to investigate the feasibility of implementing these suggestions.



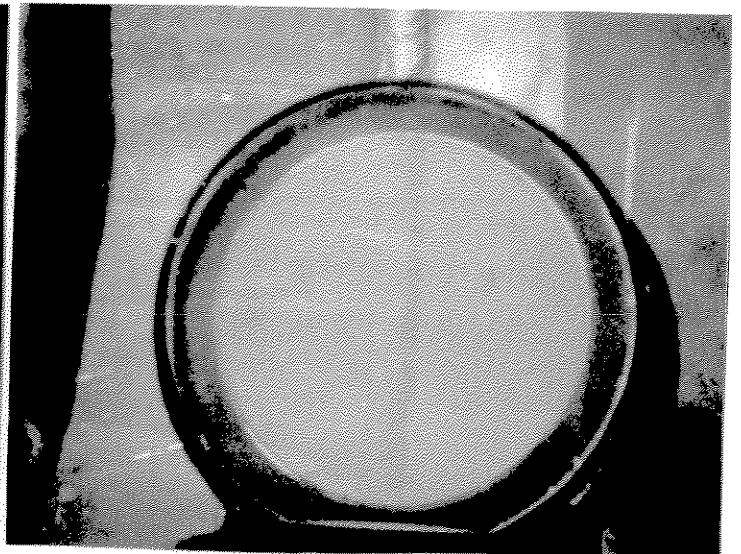
(a) Image of machined slot.



(b) Image of a visible crack.



(c) Image of a visible crack.



(d) Image of a raised weld bead.

Figure 14. Data collected by Mr. John Rudlin from the Underwater NDE Centre affiliated with the of University College London. These images were made using the Phase II prototype imager. All of the defects imaged were visible.

### Task 6 - Final Report.

The objective of Task 6 is to prepare this final report detailing the work accomplished under the program and make recommendations for further investigation.

## CONCLUSIONS AND RECOMMENDATIONS

We were generally encouraged by the results of the Underwater NDE Centre tests. These tests indicated that our Magneto-Optic imager is applicable to underwater inspection. However, we were disappointed with the inability of the imager to detect circumferential cracks on small diameter piping or cracks in the vicinity of a weld bead. The problem in both these situations is lift-off (the distance between the sensor and the surface being inspected). Because a) the garnet film used in the imager is rigid and b) sensitivity diminishes rapidly with lift-off, this constitutes an intractable problem with this design. The ideal sensor for this application would be sufficiently flexible to conform to small diameter piping and to accommodate rough surfaces such as welded joints in the "as welded" condition.

Based on the results of our preliminary work on liquid crystal sensors, we feel that this approach may offer a better solution to the underwater inspection problem than an imager based on garnet film. These designs have the potential for fielding flexible sensors which can conform to curved test objects. We therefore recommend that the Department of Transportation consider funding additional work on liquid crystal sensors. Failure Analysis Associates would be happy to provide a detailed proposal to the DOT describing a research project with the goal of demonstrating such a sensor.

## REFERENCES

1. 'Nondestructive Testing - A Survey', National Aeronautics and Space Administration Technology Utilization Report, NASA SP-5113 (1973).
2. A. H. Eschenfelder, Magnetic Bubble Technology, Springer-Verlag, new York (1980).
3. G. R. Pulliam, W. E. Ross, B. MacNeal, and R. F. Bailey, 'Large Stable Magnetic Domains', J. Appl. Phys., 53, 2754 (March 1982).
4. G. B. Scott and D. E. Locklison, 'Magneto-Optic Properties and Applications of Bismuth Substituted Iron Garnets', IEEE Transactions on Magnetics, MAG-12 (July 1976).
5. G. L. Fitzpatrick, 'Imaging Near Surface Flaws in Ferromagnetic Materials Using Magneto-Optic Detectors', Review of Progress in Quantitative Nondestructive Evaluation, Plenum Press (1985).
6. G. L. Fitzpatrick, 'Direct Flux Leakage Imaging', Journal of Nondestructive Testing Communications, Gordon and Breach (1985).
7. G. L. Fitzpatrick, 'Imaging Near-Surface Flaws in Ferromagnetic Materials', Eleventh Work Conference on Nondestructive Testing, ASNT (1985).

**Appendix A**

Test Report from Underwater NDE Centre  
University College London



## Report on Use of Magneto-Optic Imager for Crack Detection in Welded Joints Underwater

### 1. Introduction

The magneto-optic imager, supplied by Failure Analysis Associates, was evaluated for the inspection of a selection of samples at the UCL Underwater NDE Centre. The samples included flat plates and tubular joints containing cracks.

### 2. Procedure

A trial to establish the optimum operating conditions (external magnetic field and internal current) was carried out for each test sample. The component was then taken into the diving tank, the tests repeated and photographs taken. The photography settings were as initially suggested by FAA, but as the exposure timing was manual, two pictures of each experiment were taken. A calibration of the device was obtained with a magnetic strip material. Details of samples on which signals were obtained were supplied to FAA. It was not possible to test any cracked tubular joints for the reasons outlined below.

### 3. Results and Discussion

#### 3.1 Flat Plate Tests

Results from the flat plate tests were supplied to FAA. These showed that cracks or slots were detectable with the instrument in this geometry. This would suggest that cracks in slightly convex surfaces may also be detectable, although the magnetic field may be more difficult to set up. The device was very sensitive to positioning of the external magnetic field, and it is suggested that an improved and simpler operation could be obtained with a field supplied from the instrument itself.

On one plate (samples) a raised weld bead obscured signals from a large slot, so the device cannot be used for crack detection with a raised weld bead.

#### 3.2 Tubular Joint Tests

Several attempts were made to inspect tubular joints but in no case was it possible to obtain signals from cracks, even when the crack was large enough to be visible with the naked eye.

The reason for this is probably that, on a tubular joint, the angle of the weld bead, and/or the angle of the joint, prevent access of the instrument to the area where the magnetic field has been disturbed by the crack. This is because the instrument has a large rigid flat area for sensing which cannot approach an internal angle.

### 3.3 Underwater Operation

No problems were experienced with underwater operation of the device other than setting up of magnetic field. The divers would need special training to operate the device, particularly with its sensitivity to the external field.

### **4. Conclusion**

The device is capable of detecting cracks in flat plates underwater, but is generally unsuitable for welded joints in the as welded condition.

### **5. Recommendations**

In order to make the device potentially more suitable for crack detection the following modifications are suggested:

- (1) Introduce an internal magnetic field.
- (2) Reduce the size of the sensing area so that it will fit into weld toes and angled joints.

UNIVERSITY COLLEGE LONDON  
UNDERWATER NDE CENTRE

SHORT FORM CATALOGUE  
OF CRACKED TUBULAR JOINTS

INCLUDING  
LIBRARY AND TRAINING SAMPLES

DOC/NDE/89/044  
Department of Mechanical Engineering  
University College London  
Torrington Place  
London WC1E 7JE

## 1. Introduction

The UCL Underwater NDE Centre has built up over a number of years a library of tubular joints containing real laboratory induced fatigue cracks. These have been divided into two groups (1) the confidential library of 80 braces containing a variety of cracked and uncracked braces in different locations. (2) a training library, consisting of a number of real fatigue cracks in cut down tubular joints for use in training programmes.

The confidential library is suitable for full scale trials and contains enough cracks to establish reliable POD curves for equipment or operators.

The training library is supplied with details of the crack and is suitable for operator training, and equipment evaluation. Transport of these nodes is relatively easy.

## 2. Crack Characterisation

The cracks are characterised by the use of MPI or techniques together with an ACPD measurement of crack depth. In certain cases ultrasonic time of flight diffraction techniques have also been used.

## 3. Fatigue Tests

In order to produce cracks in the tubular welded joints these joints must be fatigued in test rigs. The nature of the fatigue test can affect the type of crack produced, its shape and direction. The fatigue loading could be high, producing long shallow cracks, or low, producing short deep cracks. They could be constant amplitude, or could have a load history representing wind and wave loadings. The fatigue test could also be carried out in air or in seawater as other specified environment. The loading could also be in different directions, for example parallel or perpendicular to the chord, axial or more complicated options. Additional variable parameters might include weld profile parent and weld materials.

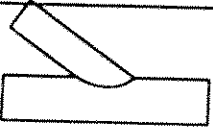
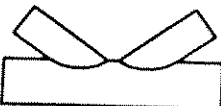
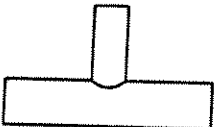
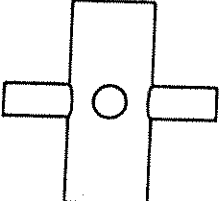
## 4. Fatigue Cracks

The provision of genuine fatigue cracks in the library enables a reliable baseline to be established for NDT methods in crack detection or sizing. Doubts as to the relationship in the performance of NDT tests between real and artificial defects are removed.

## 5. Equipment

The currently available equipment at the Underwater NDE Centre laboratory at City University consists of 4 actuators up to 500 KN capacity. Additional capacity also exists at UCL for continuous monitoring of tests, and computer driven load histories.

# TRAINING NODE SAMPLES

	No	CHORD		BRACE	
		dia	W.T	dia	W.T
	2	450	16	324	12
	1	450	16	324	12
	5	450	16	324	12
	1	800	32	324	16



## UNDERWATER NDE CENTRE

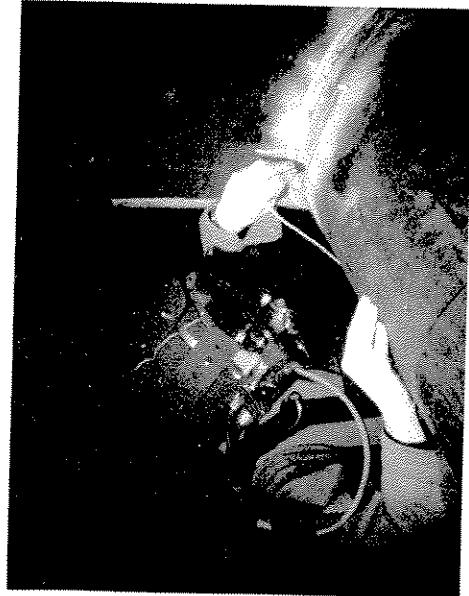
University College London

### RELIABILITY OF UNDERWATER INSPECTION TECHNIQUES

Once established, the Centre began studies on inspection techniques commonly used offshore. Initially, work started on those procedures which basically locate defects. Now, techniques which not only detect defects, but also measure their length and depth are being examined. The trials are conducted by experienced North Sea diver inspectors who perform 'blind', i.e. they have no knowledge of the defect, its location, or even if one is present in the weld under examination.

The technique most widely used offshore is Magnetic Particle Inspection (MPI). Considerable effort was spent in establishing an Inspection Procedure for MPI. This has to be closely adhered to during the trials to provide a sound basis by which its accuracy can be established. Success is measured by comparison of the 'indication' with the known defect. When statistically assessed, success can be quantified in terms of Probability of Detection, and presented in the form of curves usually showing how success rate varies with defect length. The level of confidence depends on the number of defects examined. Twenty eight need to be successfully detected to demonstrate a 90% POD at a 95% level of confidence as in the aerospace and nuclear industry.

Eddy Current (EC) procedures were examined next. A closely related technique, alternating current potential drop (ACPD) is also being studied while time-of-flight diffraction and ultrasonic creeping wave will be considered in the near future.

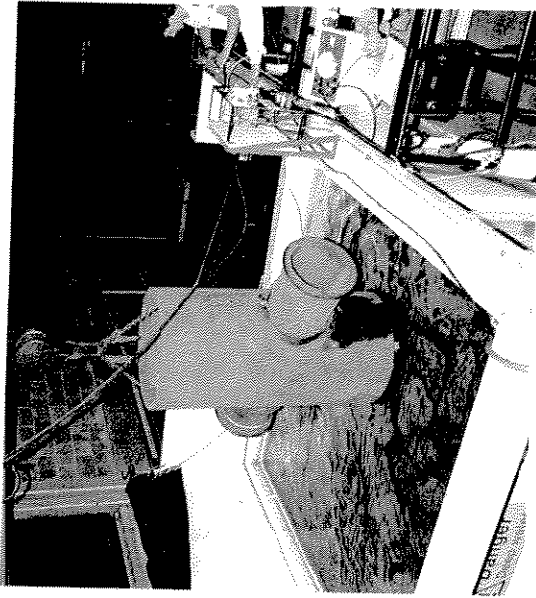


### BACKGROUND

The Underwater NDE Centre was initiated in 1982 when the Offshore industry indicated that there was a special need to evaluate the reliability of underwater inspection techniques. With the annual cost of inspection in the North Sea running at some £25 million, it is clearly essential that it be conducted effectively. However, experience in the aircraft and nuclear industries 'had revealed inspection procedures were far less effective than had been believed. Given the nature of fatigue damage in North Sea structures, and the hazardous environment, it is important to be able to detect and size defects efficiently and effectively so that repair strategies can be rationally planned. Information on inspection reliability is very important in this procedure.

The Science and Engineering Research Council through Marine Technology Directorate, Department of Energy and Industry responded to the need and the Centre was established on a 'Club' basis. The facilities provided were a diving tank, fatigue testing machines, and a confidential library of pre-cracked full scale tubular joints -- these are described in detail elsewhere in this brochure. The equipment was erected indoors at The City University, in a co-operative venture, because of ease of access to their large laboratories.

### FACILITIES



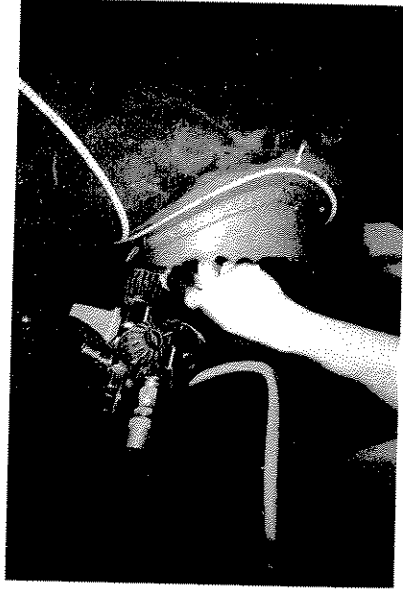
### DIVING TANK

The tank is 5m x 4.5m x 5m deep with viewing ports and a viewing/control platform level with the top of the tank. The water is continuously filtered and can be heated to 40°C. Diving support via a surface air supply is available for two inspectors with full diver surface 'hard-wire' communications. The tank is served by a 5 tonne overhead crane.

### FATIGUE TESTING MACHINES

The Centre's activities have concentrated on developing a library of pre-cracked welded tubular joints. For the numbers and schedule involved, this has been most effectively done in-house. Accordingly, suitable actuators and rigs were installed. The Centre now has three rigs for producing defects covering a variety of nodal configurations and sizes. The present maximum capacity is  $\pm 250\text{kN}$ .

The Centre acknowledges the contributions of Instron (UK) Limited in helping to establish these particular facilities.



## UNIQUE LIBRARY OF PRE-CRACKED WELDED TUBULAR JOINTS



To provide a basis for independently assessing the accuracy of inspection procedures, it is necessary to institute a confidential library of defects. This has been the main objective of the Centre and the library is now well established.

The desired range of defect sizes was defined by the Centre Steering Committee. The defects are the result of the fatigue tests and are only known to Centre staff. They have been carefully located and measured so now can be used to quantify both Probability of Detection and Sizing of inspection techniques.

The library consists of a wide variety of node shapes, generally symmetrical in order not to be recognised by the experienced North Sea Inspector Divers who perform the inspection trials. When complete the library will contain some 153 defects of lengths varying from 2 to over 300mm with depths up to 25mm. Some braces are defect free in order to ensure that diver expectations do not influence inspections.

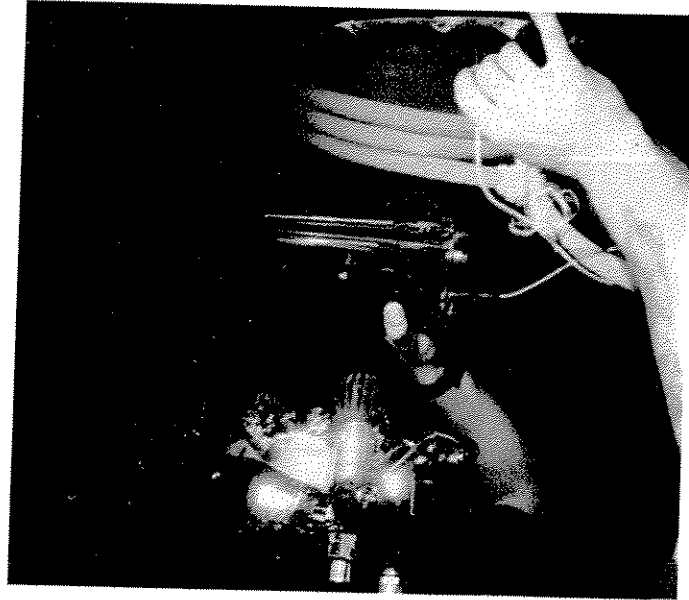
## INDEPENDENT TRIALS AND EQUIPMENT EVALUATION

The facilities within the Centre, viz, fatigue rigs, diving tank and library, are available to any organisation wishing to carry out similar activities as presently performed in-house. Thus, fatigue tests can be set up followed by relevant underwater inspections. Alternatively, the library can be used as a source of defects. British Gas Corporation have found the Centre a useful proving place for equipment they are developing.

The Centre Staff are well experienced in using underwater inspection techniques, and in the interpretation of equipment output, whether visual or digital.

The Centre staff are available for consultation concerning inspection-related needs and problems. In particular, our Diving Supervisor can also organise teams of divers with general or specialist inspection skills for on-site trials.

The Centre wishes to acknowledge the assistance of British Gas Corporation, in supplying photographs for this pamphlet.



## WHO TO CONTACT

The Director: **Professor W. D. Dover**  
The Manager: **Dr. Paul Frieze**



**UNDERWATER NDE CENTRE**  
Mechanical Engineering Department,  
University College London,  
Torrington Place,  
London WC1E 7JE.  
Telephone 01-380 7183/4.  
Fax 01-388 0100.  
Telex 296273.

The Diving Supervisor: **Peter Sieniewicz**  
Engineering and technical staff.

**UNDERWATER NDE CENTRE**  
Mechanical Engineering Department,  
The City University,  
Northampton Square,  
London EC1V 0BH.  
Telephone 01-253 4399 ext. 4212.  
Telex 263896.

## RELATED ACTIVITIES

### MSc

The Mechanical Engineering Department of University College London offers a part-time MSc course in NDE. Contacts **Dr. Len Bond**, 01-387 7050 ext 3944 or **Dr. Roy Collins**, ext. 3925.

### NON-CONTACTING ELECTROMAGNETIC DEVICES

A unit closely linked to the Centre at University College has been studying the nature of the electromagnetic fields associated with defects in materials containing induced or injected currents. This has led to the situation where it is now possible to predict from theory the nature of the fields and to interpret measurements of the magnetic distribution in terms of defect size. Non-contacting probes based on this development have been produced and these are now available for detection and sizing.

Contact: **Dr. Roy Collins** or **Dr. Martin Lugg**,  
01-380 7182.